catalysts

MDPI

Article

Improving Product Yield in the Direct Carboxylation of Glycerol with CO_2 through the Tailored Selection of Dehydrating Agents

Nurul Razali [1,2] and James McGregor [2,*]

[1] Faculty of Ocean Engineering Technology and Informatics, Universiti Malaysia Terengganu, Kuala Terengganu 21300, Malaysia; nrazali01@gmail.com
[2] Department of Chemical and Biological Engineering, University of Sheffield, Mappin Street, Sheffield S1 3JD, UK
* Correspondence: james.mcgregor@sheffield.ac.uk; Tel.: +44-114-222-4918

Abstract: Improved yields of, and selectivities to, value-added products synthesised from glycerol are shown to be achieved through the judicious selection of dehydrating agents and through the development of improved catalysts. The direct carboxylation of glycerol with CO_2 over lanthanum-based catalysts can yield glycerol carbonate in the presence of basic species, or acetins in the presence of acidic molecules. The formation of glycerol carbonate is thermodynamically limited; removal of produced water shifts the chemical equilibrium to the product side. Acetonitrile, benzonitrile and adiponitrile have been investigated as basic dehydrating agents to promote glycerol carbonate synthesis. In parallel, acetic anhydride has been studied as an acidic dehydrating agent to promote acetin formation. Alongside this, the influence of the catalyst synthesis method has been investigated allowing links between the physicochemical properties of the catalyst and catalytic performance to be determined. The use of acetonitrile and La catalysts allows the results for the novel dehydrating agents to be benchmarked against literature data. Notably, adiponitrile exhibits significantly enhanced performance over other dehydrating agents, e.g., achieving a 5-fold increase in glycerol carbonate yield with respect to acetonitrile. This is in part ascribed to the fact that each molecule of adiponitrile has two nitrile functionalities to promote the reactive removal of water. In addition, mechanistic insights show that adiponitrile results in reduced by-product formation. Considering by-product formation, 4-hydroxymethyl(oxazolidin)-2-one (4-HMO) has, for the first time, been observed in all reaction systems using cyanated species. Studies investigating the influence of the catalyst synthesis route show a complex relationship between surface basicity, surface area, crystallite phase and reactivity. These results suggest alternative strategies to maximise the yield of desirable products from glycerol through tailoring the reaction chemistry and by-product formation via an appropriate choice of dehydrating agents and co-reagents.

Keywords: glycerin; carbon dioxide; La_2O_3; glycerol; carbonates; acetins

Citation: Razali, N.; McGregor, J. Improving Product Yield in the Direct Carboxylation of Glycerol with CO_2 through the Tailored Selection of Dehydrating Agents. *Catalysts* **2021**, *11*, 138. https://doi.org/10.3390/catal11010138

Received: 22 December 2020
Accepted: 12 January 2021
Published: 18 January 2021

1. Introduction

Glycerol is a by-product of biodiesel synthesis, 10 wt.% of glycerol is produced for every kilogram of biodiesel, and glycerol produced in this way contributes to ~67% of glycerol manufactured globally [1]. The increasing commercialisation of biodiesel is forecast to generate surplus glycerol, depressing its market value [2]. Greater utilisation of glycerol as a chemical feedstock therefore represents a key opportunity in the chemicals sector. Potential products which can be synthesised include glycerol carbonate and acetins. Glycerol carbonate has desirable properties such as low flammability, biodegradability, is non-toxic and has a high boiling point. These make it suitable for a wide range of applications including as an electrolyte in lithium-ion batteries, as a solvent and in surfactants [3]. Acetins are commercially valuable fuel additives, in particular for biodiesel (and hence their synthesis from a by-product of biodiesel production is particularly attractive). Triacetin

also has additional applications in cosmetics, pharmaceuticals and food industries [4–6]; it has also been suggested as a source of food energy on space missions [7].

Approximately 20 Mt of linear and cyclic carbonates are produced from the cycloaddition of CO_2 and epoxides annually [8]. Glycerol carbonate can be manufactured from the reaction of glycerol with phosgene or via a transesterification reaction of acyclic organic carbonates (e.g., dimethyl or diethyl carbonate) [9]. These carbonates are commonly produced from phosgene. Phosgene is considered as toxic, environmental unfriendly and highly corrosive. The use of phosgene is therefore being eliminated and is banned in several countries [10]. Alternatively, glycerol carbonate can be synthesised from carbonylation of glycerol with urea [11–13]. This reaction has gained much interest among researchers because urea is available at a low-cost and this reaction can be carried out in the absence of a solvent; nevertheless, environmentally unfriendly by-products including isocyanic acid and biuret are produced and the elimination of ammonia during reaction is required [14–16].

The reaction of glycerol with CO_2 is a promising alternative route to synthesise glycerol carbonate [17,18]. CO_2 concentration in the atmosphere is significantly increasing and reached 416 ppm in June 2020 [19]; therefore, it is important to utilise the highly available and low-cost CO_2 which contributes directly to climate change. The reaction of glycerol and CO_2 can therefore be considered as a 'green' process; however it is thermodynamically limited [20], exhibiting a relatively low chemical equilibrium constant: 1.3×10^{-3} at 160 °C and 50 bar [21]. Elevated temperatures and high pressures (>50 bar) are therefore typically employed.

In order to overcome thermodynamic limitations, basic dehydrating agents can be used to remove water and shift the equilibrium to the product side. In the absence of dehydrating agents, the reaction achieves only low yields, e.g., over metal impregnated zeolites, at 100 bar, a 6% yield of glycerol carbonate was achieved [22]; while an 8% yield of glycerol carbonate was observed upon the introduction of ZnO at 150 bar [23]. Higher yields have been achieved when conducting the reaction in methanol as a solvent, with George and co-workers observing a 35% yield at 138 bar [24]. The dehydrating agent most commonly applied in glycerol carbonate synthesis is acetonitrile [25–29].

In contrast, in the presence of an acid, such as acetic acid, glycerol can be transformed into acetins. Monoacetin (2,3-dihydroxypropyl acetate) can be produced in the absence of a catalyst. Diacetin (1,2,3-propanetriol, 1,2-diacetate) and triacetin (1,2,3-triacetoxypropane) are however the more desirable products as fuel additives: they enhance the octane rating; improve the cold flow and viscosity properties; and reduce the fuel cloud point of biodiesel [6]. Most production of di- and triacetin involves a two-step process whereby glycerol reacts with acetic acid to form predominately monoacetin, followed by catalytic esterification of monoacetin with acetic anhydride to form the desired products. Sandesh and co-workers have investigated a one-step process using acetic anhydride and employing a caesium phosphotungstate catalyst at 30 °C, achieving a yield of ~99% to di- and triacetins [5]. Konwar et al. achieved similar yields over zeolite catalysts at 100 °C [4].

When glycerol carbonate synthesis is conducted in the presence of acetonitrile, the dehydrating agent may be hydrolysed into acetic acid. Similar to the intentional production of acetins, *vide supra*, esterification of glycerol and acetic acid may then occur. Hydrolysis of acetonitrile in situ produces mono-, di- and triacetin as by-products. This has the effect to reduce the overall selectivity to glycerol carbonate. Alternative dehydrating agents have therefore been the subject of investigation. For instance, Liu et al. employed 2-cyanopyridine at 40 bar and 150 °C, resulting in a 20% yield of glycerol carbonate with 2-picolinamide as the by-product [30]. The application of adiponitrile as an alternative dehydrating agent has recently been reported for the first time, using crude glycerol as the feedstock [1]. In that work however, no attempt was made to experimentally compare the reactivity in the presence of adiponitrile with that in the presence of other dehydrating agents. Adiponitrile is expected to present advantages over acetonitrile in that it is a dicyanated molecule and hence is likely to be a more effective chemical water trap.

The present work aims at developing a more complete understanding of the role of different types of dehydrating agent/co-reactant on the conversion of glycerol in the presence of carbon dioxide and a catalyst. A key focus is on developing a process which can operate at mild conditions of moderate temperature and pressure and at low catalyst concentrations. Experimental investigations using a range of dehydrating agents are benchmarked against results obtained using acetonitrile, in order to facilitate comparisons with the existing literature. This would otherwise be challenging, as there is wide variation in the reaction conditions employed in previous research. The focus is therefore not on developing an optimised catalytic system but on providing novel insights into the behaviour of dehydrating agents. These can then be accounted for when developing advanced and innovative catalysts and catalytic processes. In addition to acetonitrile, exemplar dehydrating agents representing acidic and mono- and dicyanated species are employed in order to relate their chemical properties to their influence on the reaction. These are acetic anhydride, adiponitrile and benzonitrile. All reactions are conducted in the absence of solvent. Additionally, the impact of the physicochemical characteristics of the catalyst on the catalytic performance were investigated. In this case, the impact of commercial La_2O_3 (C-La_2O_3) was also analysed along with the catalysts prepared in-house. $La_2O_2CO_3$-based catalysts were prepared via co-precipitation (CP-$La_2O_2CO_3$), hydrothermal (HT-$La_2O_2CO_3$) and sol-gel (SG-$La_2O_2CO_3$) methods, yielding materials with differing properties. $La_2O_2CO_3$ catalysts have been previously investigated and hence provide a baseline with which to compare the results generated herein with prior studies [1,26].

2. Results and Discussion

2.1. Catalyst Characterisation

C-La_2O_3, CP-$La_2O_2CO_3$, SG-$La_2O_2CO_3$ and HT-$La_2O_2CO_3$ were characterised using scanning electron microscopy (SEM) and analysed using ImageJ software in order to determine their morphology at the macro-scale (Figure 1). Each catalyst shows an irregular shape and particle size. CP-$La_2O_2CO_3$ and HT-$La_2O_2CO_3$ have larger particle sizes (typically 3–10 µm, Figure S1) when compared with C-La_2O_3 (~1 µm) and SG-$La_2O_2CO_3$ (~3 µm). Additional analysis techniques are conducted to provide quantitative information to facilitate the establishment of structure-performance relationships. Brunauer–Emmett–Teller (BET) measurements of C-La_2O_3 determined a surface area of 13.6 m^2/g, considerably lower than for CP-$La_2O_2CO_3$ (60.7 m^2/g), SG-$La_2O_2CO_3$ (194.0 m^2/g) and HT-$La_2O_2CO_3$ (27.9 m^2/g) (Table 1). The pore volume and the average pore diameter were determined from the desorption branch of the isotherm via the Barrett-Joyner-Halenda (BJH) method. CP-$La_2O_2CO_3$ showed a larger pore volume (0.3 $cm^3 \cdot g^{-1}$) and average pore diameter (13.8 nm) in comparison to SG-$La_2O_2CO_3$ and HT-$La_2O_2CO_3$ (Table 1). This is likely to favour the diffusion of the reactants and products to and from the catalyst.

Table 1. BET surface area, pore volume, average pore diameter and total number of basic sites of the catalysts.

Catalyst	[a] BET Surface Area ($m^2 \cdot g^{-1}$)	[b] Pore Volume ($cm^3 \cdot g^{-1}$)	[b] Average Pore Diameter (nm)	[c] Crystallite Size (nm)	[d] Total Basic Site ($mmol_{CO2} \cdot g^{-1}$)
C-La_2O_3	13.6	0.1	3.1	37	0.8
CP-$La_2O_2CO_3$	60.7	0.3	13.8	31	1.5
SG-$La_2O_2CO_3$	194.0	0.2	2.2	N/A	1.6
HT-$La_2O_2CO_3$	27.9	0.1	8.8	27	1.4

[a] BET surface area, [b] Measured from the desorption branch according to the BJH method, [c] Determined by X-ray diffraction (XRD) using the Scherrer equation, [d] Measured using CO_2-temperature programmed desorption (TPD).

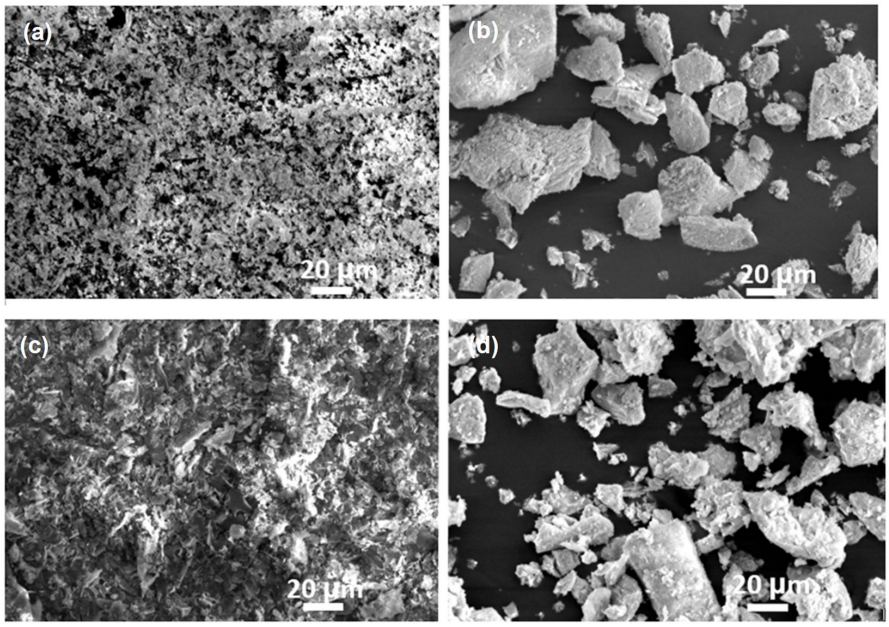

Figure 1. SEM micrographs of (**a**) C-La_2O_3, (**b**) CP-$La_2O_2CO_3$ (**c**) SG-$La_2O_2CO_3$ and (**d**) HT-$La_2O_2CO_3$. Magnification is 250 × collected with an acceleration voltage of 20 kV.

The basicity of the catalyst was analysed using TPD-CO_2 from 30 to 900 °C. The data are summarised in Table 1. It is notable that the number of basic sites and the total amount of desorbed CO_2 is not strongly influenced by the method of catalyst preparation, with all $La_2O_2CO_3$ prepared in-house exhibiting > 1.4 mmol of CO_2 per gram of catalyst. C-La_2O_3 in contrast, presents a value of 0.8 $mmol_{CO2}$ g^{-1}.

X-ray diffraction (XRD) has been employed in order to investigate the crystalline phases of C-La_2O_3 and the $La_2O_2CO_3$-based catalysts (Figure 2). Crystallite sizes were calculated using the Scherrer equation. The largest crystallite size, 37 nm (30.2°, hexagonal La_2O_3), was calculated for C-La_2O_3. CP-$La_2O_2CO_3$ and HT-$La_2O_2CO_3$ were calculated to possess crystallite sizes of 31 nm (30.3°, hexagonal $La_2O_2CO_3$) and 27 nm (30.4°, monoclinic $La_2O_2CO_3$) respectively. Crystalline structures of $La_2O_2CO_3$ can be categorised into three different types (types I, Ia, and II), which are formed depending on the location of $La_2O_2^{2+}$ and CO_3^{2-} ions [31]. Type I consists square layers of $La_2O_2^{2+}$ ions in a tetragonal crystalline form separated by CO_3^{2-} ions. Type Ia is the monoclinic distortion of type I, and type II is a hexagonal crystalline structure of La oxycarbonate [31].

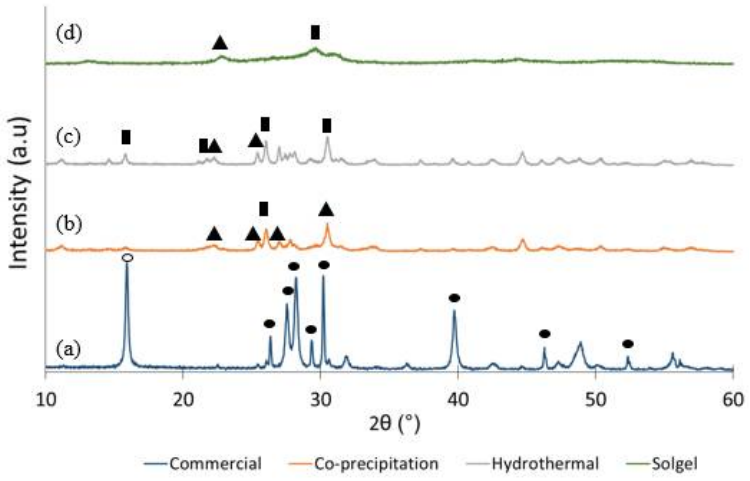

Figure 2. XRD patterns of (**a**) C-La_2O_3, (**b**) CP-$La_2O_2CO_3$, (**c**) HT-$La_2O_2CO_3$ and (**d**) SG-$La_2O_2CO_3$. (O) $La(OH)_3$, (●) hexagonal La_2O_3, (▲) hexagonal $La_2O_2CO_3$ and (■) monoclinic $La_2O_2CO_3$.

Peaks at 22.5, 25.4, 27.0 and 30.4° are characteristic of monoclinic $La_2O_2CO_3$ (JCPDS 48-1113), while peaks at 15.7, 21.4, 25.8 and 29.4° are ascribed to hexagonal $La_2O_2CO_3$ (JCPDS 37-0804). From the XRD data, the major crystalline fraction of CP-$La_2O_2CO_3$ exists in the hexagonal crystal phase, while the major component of HT-$La_2O_2CO_3$ is the monoclinic crystal phase. C-La_2O_3 exists in a hexagonal crystal phase (JCPDS 73-2141) [32,33]. The peak at 15.9° is ascribed to $La(OH)_3$ [29,34]. C-La_2O_3 is highly sensitive to atmospheric water [35,36], thus the interaction of La_2O_3-C with moisture in atmosphere promotes the formation of $La(OH)_3$ [37]. No strong diffraction peaks are observed for SG-$La_2O_2CO_3$, indicating that it exists in an amorphous state. $La_2O_2CO_3$-based catalysts were calcined at 400 °C and no peak was detected at 15.9°. The structural properties of the catalyst are therefore highly dependent on the catalyst preparation method.

The solid catalysts were also characterised by using Fourier transform infrared (FTIR) spectroscopy as shown in Figure 3. The peak at 3607 cm^{-1} in the spectrum of C-La_2O_3 is indicative of the presence of bulk -OH functional groups, supporting the conclusion from XRD that $La(OH)_3$ forms in the presence of atmospheric moisture. The peaks at 1508 and 1460 cm^{-1} show that the catalyst surface has reacted with CO_2 and water to form chemisorbed carbonate and bicarbonates [38]. C-La_2O_3 is sensitive to atmospheric CO_2. The peak at 844 cm^{-1} is ascribed to carbonate groups [36].

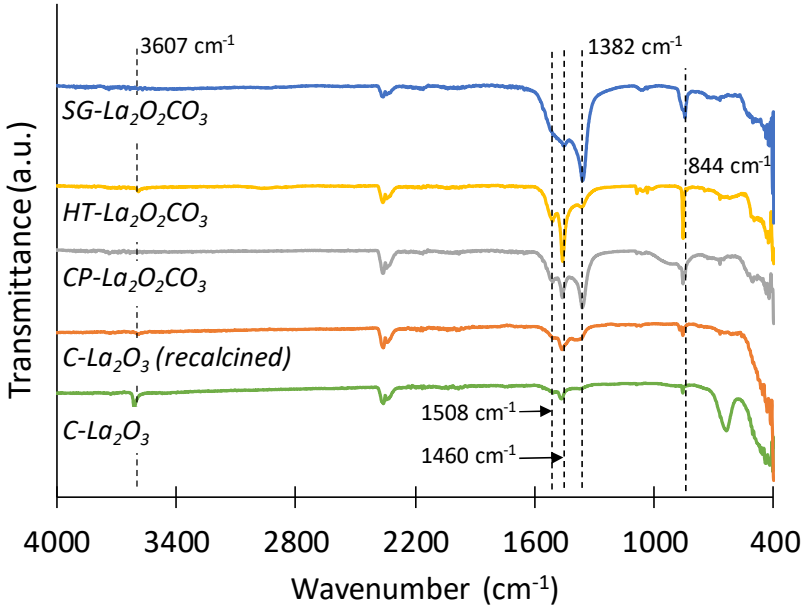

Figure 3. FTIR spectra of C-La_2O_3 and calcined C-La_2O_3 and $La_2O_2CO_3$ catalysts prepared via co-precipitation (CP), sol-gel (SG) and hydrothermal (HT) methods.

2.2. Impact of Dehydrating Agents

The influence of the four dehydrating agents—acetic anhydride, acetonitrile, benzonitrile and adiponitrile—on the conversion of glycerol in the presence of CO_2 was investigated over C-La_2O_3. A "blank" run was also conducted in the absence of both a dehydrating agent and a catalyst, in which a conversion of only 1.4% was observed, with no glycerol carbonate or acetin production (Table 2). The impact of the dehydrating agents on glycerol conversion decreased in the order: acetic anhydride (97%) > benzonitrile (71%) > adiponitrile (58%) > acetonitrile (48%). Considering the basic dehydrating agents, adiponitrile provides the highest selectivity to glycerol carbonate (17%), followed by benzonitrile (5%) and acetonitrile (4%). The enhanced selectivity for adiponitrile is in part ascribed to the fact that each molecule of the dehydrating agent has two nitrile functionalities, rendering it more effective as a chemical water trap when compared to monocyanated species such as acetonitrile and benzonitrile.

Table 2. The influence of dehydrating agents on glycerol conversion and selectivity to desired products. Reaction conditions: p = 45 bar, 6 wt.% C-La_2O_3, 22.5 mmol glycerol, 45 mmol dehydrating agent, 18 h and reaction temperature = 160 °C.

Dehydrating Agent	Properties	Conversion of Glycerol (%)	Products Selectivity (%)			
			Glycerol carbonate	*Monoacetin*	*Diacetin*	*Triacetin*
[a] Blank	–	1	0	0	0	0
Acetic anhydride	Acidic	97	0	17	60	24
Acetonitrile	Base (Monocyanated)	48	4	12	3	0
Benzonitrile	Base (Monocyanated)	71	5	0	0	0
Adiponitrile	Base (Dicyanated)	58	17	0	0	0

[a] absence of catalyst and dehydrating agent.

While both monocyanated agents (acetonitrile and benzonitrile) present similar glycerol carbonate selectivities, they result in very different conversions of glycerol. The conversion achieved in the presence of benzonitrile is 71%, as compared to only 48% with acetonitrile; this is despite the higher basicity of acetonitrile. The high conversion achieved with benzonitrile is in agreement with previous studies on a closely related reaction where benzonitrile was employed as a dehydrating agent in the production of propylene carbonate from propylene glycol and carbon dioxide [39]. The origins of this effect are ascribed to the greater solubility of CO_2 in benzonitrile cf. acetonitrile, thereby facilitating transfer of CO_2 to the catalyst surface and subsequent activation and reaction. The molecular diameters of carbon dioxide, glycerol and glycerol carbonate are 0.33, 0.52 and 0.65 nm respectively [40,41]. Therefore, based on the data shown in Table 1, mass transfer of the reactant within the catalyst pores is expected to be relatively facile; it is therefore more likely that mass transfer between the gas-phase (CO_2) and the catalyst surface in the liquid (glycerol) phase is the dominant transport effect. The carboxylation of glycerol in the presence of benzonitrile produces glycerol carbonate, with water as the by-product. If subsequent hydrolysis of benzonitrile occurred, then this would produce benzamide and benzoic acid as secondary products. However, neither benzamide nor benzoic acid were detected by gas chromatography-mass spectrometry (GC-MS) after 18 h of reaction. It is hence concluded that no esterified products were formed from this reaction. Despite this, and the lack of formation of acetins as by-products, selectivity to glycerol carbonate is only 5%. The largest peak, by area, in the GC-MS chromatogram is unidentified (reference to the NIST spectral library does not identify a suitable match). However characteristic fragments associated with a phenyl group (m/z = 77) and glycerol derivatives (m/z = 45) are identified. This species can therefore be assigned to the product of a reaction between benzonitrile and either glycerol or a glycerol derived species such as glycerol carbonate. The fragmentation pattern of this species is shown in Table S1.

The low selectivity to glycerol carbonate when acetonitrile is employed as the dehydrating agent (4%) correlates with the formation of acetins. Selectivities of 12 and 3% to mono- and diacetin were obtained, although no triacetin was observed. Hydrolysis of acetonitrile in the reaction of CO_2 and glycerol has been described in several reports in which the hydrolysis of acetonitrile produces acetamide that is then transformed into acetic acid [26]. Acetic acid can subsequently react with glycerol, forming mono- and diacetin as described in Section 1. Acetylation of glycerol and acetic acid to mono- and diacetin is thermodynamically favourable, but triacetin production is unfavourable due to the endothermic nature of this process (Figure 4) [42,43]. In the present work, previously unreported products including 4-hydroxymethyl(oxazolidin)-2-one ($C_4H_7NO_3$, 4-HMO) have been identified in all reactions employing cyanated dehydrating agents. The carboxylation reaction in the presence of benzonitrile and acetonitrile produces 1.5- and 3-fold of the quantity of 4-HMO as compared with adiponitrile (Table S2). This reinforces the exceptional selectivity to glycerol carbonate obtained in the presence of adiponitrile. Further investigation is crucial to confirm the influence of the nitrile-based dehydrating agents on this reaction pathway.

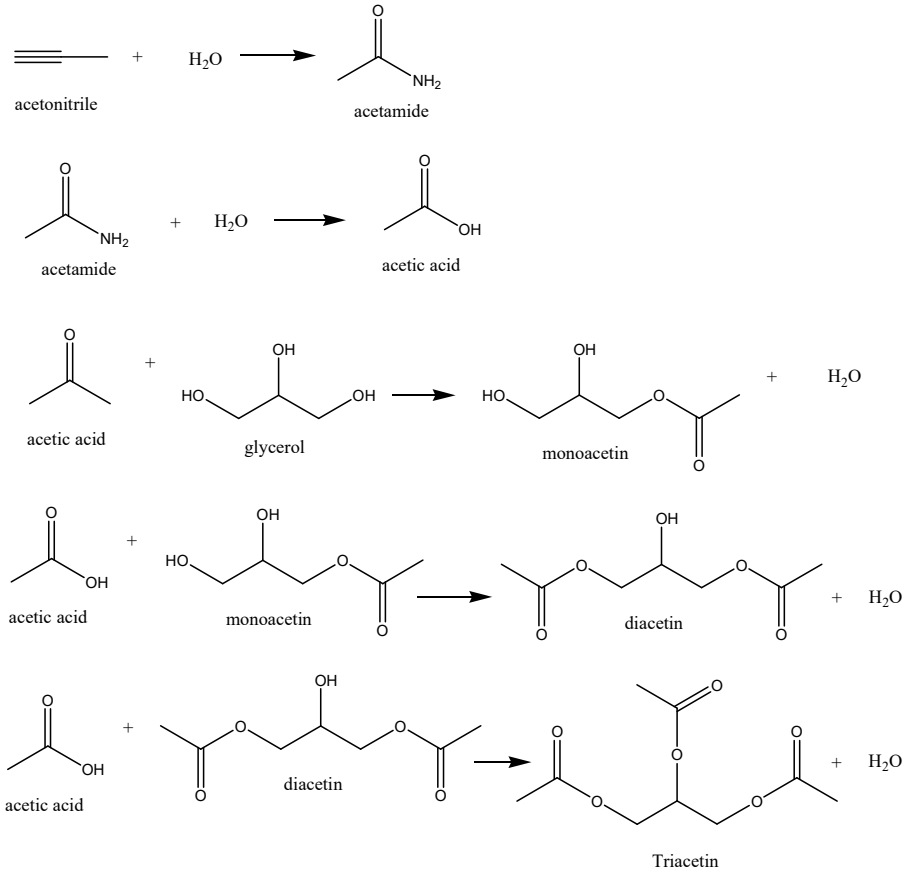

Figure 4. Reactions of glycerol and acetonitrile for the formation of mono-, di- and triacetin.

Figure 5 shows attenuated total reflection (ATR) FTIR spectra for liquid samples arising from the reaction of glycerol and CO_2 in the presence of acetonitrile, benzonitrile and adiponitrile. All spectra show a strong band at 1662 cm^{-1} ascribed to C=O in an amide linkage, indicative of the presence of a product of a secondary reaction between glycerol carbonate and the nitrile (Figure 5) [11]. This supports and adds to the conclusions from the interrogation of the mass spectra of unidentified peaks in the GC-MS chromatogram, *vide supra*. The spectrum deriving from the reaction with acetonitrile has the strongest intensity in this region. This therefore suggests that while low selectivity to glycerol carbonate is observed for this system, glycerol carbonate is produced but then rapidly converts to an amide product. Peaks at 1730 and 1790 cm^{-1}, identified in all spectra, are suggestive of the presence of C=O in a five membered cyclic ring. The peak at 1790 cm^{-1} is associated with glycerol carbonate, and that at 1730 cm^{-1} indicates the presence of 4-HMO [11], again in agreement with GC-MS results. The high intensity of the peak detected at 1730 cm^{-1} when using acetonitrile as the dehydrating agent indicates that this reaction favours the formation of 4-HMO (Figure 6). This is in line with GC-MS data which showed that in the presence of acetonitrile 4-HMO was produced in quantities two- and three-times greater than with benzonitrile and adiponitrile respectively (Table S2).

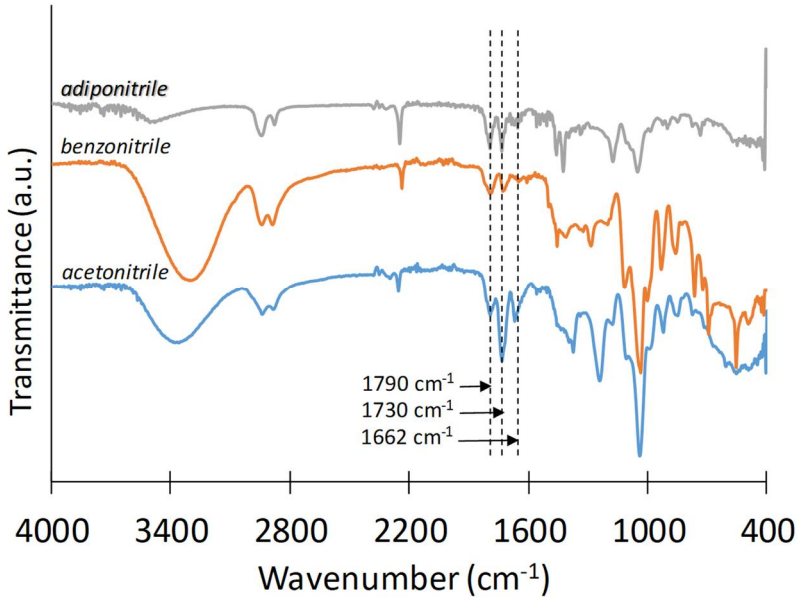

Figure 5. ATR-FTIR spectra from 4000–400 cm^{-1} of the liquid-phase resulting from the carboxylation of glycerol in the presence of different dehydrating agents: adiponitrile; benzonitrile; and acetonitrile. Reaction conditions: Reaction pressure = 45 bar, 6 wt.% C-La_2O_3 to glycerol ratio, 22.5 mmol glycerol, 45 mmol dehydrating agent, 18 h and reaction temperature = 160 °C.

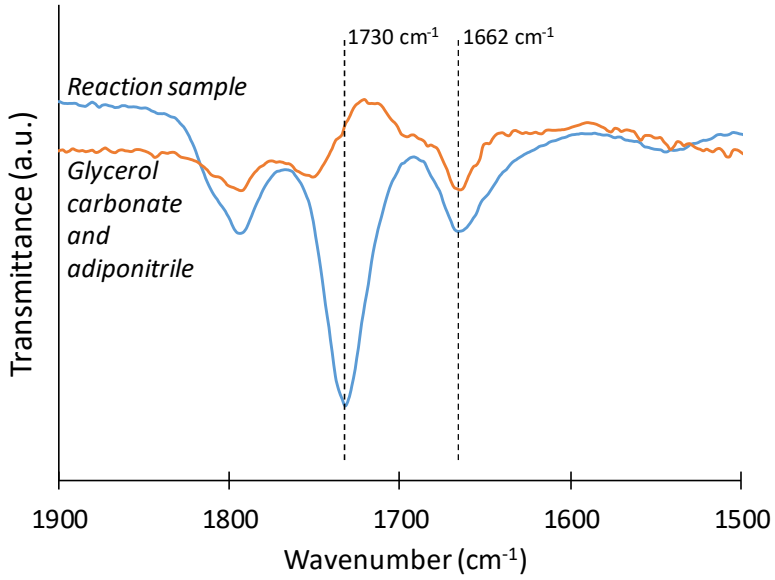

Figure 6. ATR-FTIR spectra from 1900–1500 cm^{-1} of the liquid-phase resulting from: the reaction of glycerol, CO_2 and adiponitrile; and the reaction of glycerol carbonate, CO_2 and adiponitrile. Reaction conditions: Reaction pressure = 45 bar, 6 wt.% C-La_2O_3 to glycerol ratio, 22.5 mmol glycerol, 45 mmol adiponitrile, 18 h and reaction temperature = 160 °C.

The formation of 4-HMO can proceed via different mechanistic routes, Figure 7. It is proposed that hydrolysis of adiponitrile produces adipamide and adipic acid where NH_3 is eliminated [26]; 2,3-dihydroxypropyl hydrogen carbonate (C1) and [2-hydroxy1-(hydroxymethyl)ethyl] hydrogen carbonate (C2) are produced when CO_2 attacks the carbon on the primary and secondary alcohol groups of glycerol. Then, reaction of NH_3 and C1 and C2 results in the formation of (2-amino-3-hydroxy-propyl) hydrogen carbonate (D1) and [1-(aminomethyl)-2-hydroxy-ethyl] hydrogen carbonate (D2) respectively. The formation

of both 4-HMO isomers (Figure 7(B1,B2)) are formed via cyclisation of D1 and D2 species.; 4-HMO is thereby produced from the reaction of glycerol, CO_2 and NH_3.

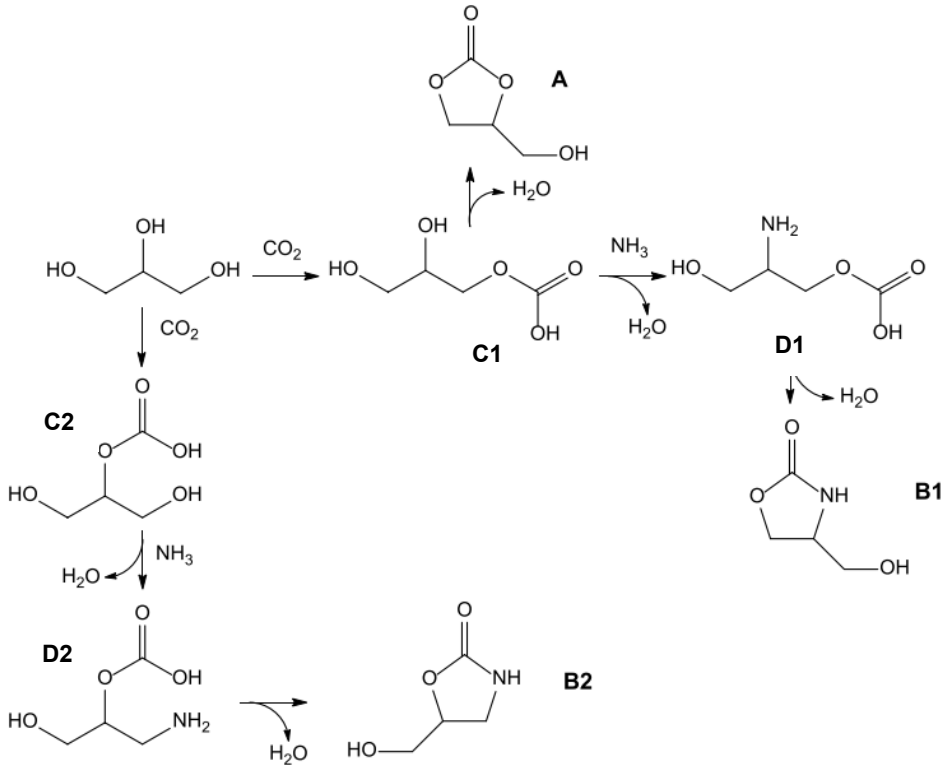

Figure 7. The proposed reaction pathway for carboxylation of glycerol to glycerol carbonate and by-products [1].

As anticipated, no glycerol carbonate was observed in the presence of the acidic dehydrating agent, acetic anhydride. This is because the acetylation of glycerol and acetic anhydride is exothermic, and favours the formation of acetins [42]. A glycerol conversion of 97% was obtained with selectivities of 17%, 60% and 23% to mono-, di- and tricaetin respectively. The combined selectivity of 84% to the more valuable di- and triacetin compares favourably with the literature, considering that no attempt was made to optimise the catalyst or reaction conditions for this process. Kong et al. have reviewed the catalytic acylation of glycerol identifying that triacetin formation is strongly affected by the acidity of the catalyst [6]. Over acidic zeolite H-beta Konwar and co-workers achieved selectivities of 38.5%, 33.2% and 28.3% to mono-, di- and triacetin respectively at 90% glycerol conversion; changing to 0%, 34.3% and 65.7% at 100% conversion [4]. Elsewhere, a cesium exchanged heteropolyacid has yielded selectivities of 13.3%, 41.2% and 45.5% to the three acetins at 98% conversion; however the use of a less acidic catalyst – sulphated zirconia – yields only 25% conversion after 120 min on stream [5].

The choice of dehydrating agent clearly exerts a significant impact on glycerol conversion and product distribution. As anticipated, acidic species favour acetin production, while basic species facilitate the formation of glycerol carbonate, in some cases alongside acetins. In the presence of adiponitrile, however, the reaction shows no activity towards acetin synthesis. This is in contrast to well-established production of these by-products in the presence of acetonitrile, corroborated by the present work. Other alternative dehydrating agents previously investigated include 2-cyanopyridine employing CeO_2 as a catalyst and dimethylformamide (DMF) as a solvent [30]. In that work, the yield of glycerol carbonate was seen to be highly dependent on the quantity of catalyst. At a catalyst loading of 18 wt.% a glycerol carbonate yield of ~10% was obtained. Herein, a yield of 17% was obtained at a much lower catalyst loading of 6 wt.% and in solvent-free conditions.

Adiponitrile therefore shows significant promise for application in the synthesis of glycerol carbonate with high selectivity and yield.

2.3. Impact of Catalyst Preparation Method

Catalytic performance in the carboxylation of glycerol to glycerol carbonate has previously been correlated with catalyst basicity [26,29,30]. CO_2 can adsorb and dissociate at basic sites, thereby facilitating reaction. In order to investigate this performance, three $La_2O_2CO_3$ catalysts were synthesised via co-precipitation, sol-gel and hydrothermal synthesis methods. As shown in Table 1, these have a higher density of basic sites on a per mass basis than the La_2O_3 catalyst employed for the reaction studies presented in Section 3.2. The basic site density of the $La_2O_2CO_3$ catalysts range from 1.4–1.6 $mmol_{CO2}$ g^{-1}, while C-La_2O_3 has a basic site density of 0.8 $mmol_{CO2}$ g^{-1}. The $La_2O_2CO_3$ catalysts also present a variety of different physicochemical properties (Table 1); notably there is a wide range of BET surface areas, ranging from 28 m^2 g^{-1} for HT-$La_2O_2CO_3$ to 194 m^2g^{-1} for SG-$La_2O_2CO_3$. Based on the results of the studies in Section 2.2, adiponitrile was selected as the dehydrating agent for this investigation into the impact of catalyst properties on catalytic performance.

Table 3 shows the glycerol conversion and selectivity to glycerol carbonate over the four different catalysts investigated. No clear correlation with surface area was observed. Among the $La_2O_2CO_3$ catalysts, CP-$La_2O_2CO_3$ shows the highest conversion and greatest selectivity, but this has the intermediate surface area of the three materials (61 $m^2 \cdot g^{-1}$). That catalytic performance does not correlate with surface area has previously been observed over CeO_2 catalysts [29,30]. However, in the present work there is a relationship between the density of basic sites on a per area basis with catalytic performance. SG-$La_2O_2CO_3$ has a similar density of basic sites on a per mass level to the other $La_2O_2CO_3$ catalysts but has a much higher surface area. It therefore has fewer basic sites per unit surface area, and hence a larger number of alternative, non-basic, surface sites available. SG-$La_2O_2CO_3$ also has the lowest selectivity to glycerol carbonate (3%) of all of the catalysts studied. In contrast, HT-$La_2O_2CO_3$ has the greatest density of basic sites per unit surface area. This catalyst, while showing improved glycerol carbonate selectivity when compared to SG-$La_2O_2CO_3$, notably shows much greater production of 4-HMO than any of the other catalysts, and specifically ~7-fold more than SG-$La_2O_2CO_3$, Table S3. In Section 2.2 it was proposed that 4-HMO is formed from a secondary reaction of glycerol carbonate.

Table 3. Reaction of glycerol and CO_2 over lanthanum-based catalysts. Reaction condition: P = 45 bar, 6 wt.% of catalyst, 22.5 mmol glycerol, 45 mmol adiponitrile, 18 h and reaction temperature = 160 °C.

Catalysts	Conversion of Glycerol	Selectivity to Glycerol Carbonate
C-La_2O_3	58.0	17.2
CP-$La_2O_2CO_3$	57.1	18.2
SG-$La_2O_2CO_3$	45.8	3.2
HT-$La_2O_2CO_3$	51.2	10.9

Amphoteric catalysts have previously been investigated for the synthesis of amines from alcohols and ammonia. Shimizu et al. showed that basic sites promoted an initial dehydrogenation step and then acidic sites catalysed a subsequent hydrogen transfer step [44]. In the context of the present work, this suggests a reaction mechanism whereby C1 and C2 in Figure 7 are converted to D1 and D2 on basic sites, followed by the conversion of D1 and D2 to 4-HMO on non-basic (acidic) sites. The increased yield of 4-HMO over HT-$La_2O_2CO_3$ may then be a consequence of it having both a high number of basic sites per g, but also a high number of alternative, non-basic, reaction sites. In contrast, the ratio of non-basic to basic sites on SG-$La_2O_2CO_3$ is much lower and hence a much lower yield of 4-HMO is obtained. It should however also be noted that SG-$La_2O_2CO_3$ exhibits differing morphological properties, having a significantly less crystalline character than the other catalysts investigated (Figure 2).

While there is no unambiguous correlation between the physical properties of the catalyst and catalyst performance it is clear that the interplay of a number of factors influences this. Most notably, the density of basic sites and the ratio of these to acidic and other adsorption sites plays a direct role in controlling reaction selectivity. Careful control of the nature and strength of adsorption sites can therefore play an important role in future catalyst design.

3. Materials and Methods

3.1. General

$La_2O_2CO_3$-based catalysts were prepared via several techniques; specifically, by co-precipitation, sol-gel and hydrothermal methods. Sodium hydroxide (97%), glycerol (99%), adiponitrile (99%), (S)-4-(hydroxymethyl)oxazolidin-2-one and mono-, di- and triacetin (technical grade, 50%) were purchased from Sigma Aldrich (Gillingham, Dorset, UK), while lanthanum nitrate hexahydrate (99%), acetonitrile (99.5%), benzonitrile (99%), acetic anhydride (99%) and glycerol carbonate (90%) were purchased from Acros Organics (Loughborough, UK). Citric acid (99%) was purchased from Alfa Aesar (Heysam, UK). The chemicals were used without any further purification and modification unless stated.

3.2. Catalyst Preparation

Commercial La_2O_3: Prior to use in the reaction, commercial La_2O_3 was calcined at 400 °C at a rate of 40 °C min^{-1} in static air. This catalyst is denoted as C-$La_2O_2CO_3$

Co-precipitation: $La_2O_2CO_3$ was prepared from $La(NO_3)_3.6H_2O$ following a similar method to that employed by Li et al. [26]. $La(NO_3)_3.6H_2O$ and 50 mL deionised water were mixed and stirred. Precipitation of $La(NO_3)_3.6H_2O$ was carried out by dropwise addition of 2 M NaOH at a constant pH of 11. The catalyst was aged at 60 °C for 4 h. The wet catalyst was centrifuged and washed with deionised water until a pH of 7 was achieved. The catalyst was then dried for 13 h at 110 °C and calcined for 5 h at 400 °C, with the synthesised catalyst denoted as CP-$La_2O_2CO_3$.

Hydrothermal: 30 mL of 6 M NaOH and 15 mL of 0.5 M $La_2(NO_3)_2.6H_2O$ were dissolved in deionised water. The mixture of both salts was then stirred vigorously for 30 min and placed in a 45 mL autoclave (Parr Instruments Model 4714; Parr Instruments, Moline, IL, USA) equipped with a magnetic stirrer. Hydrothermal treatment then took place for 22 h under constant stirring. The resultant wet catalyst was centrifuged and washed with deionised water. Finally, the catalyst was dried at 110 °C and calcined at 400 °C for 5 h, with the synthesised catalyst denoted as HT-$La_2O_2CO_3$.

Citrate sol-gel: 50 mL of both 0.5 M $La_2(NO_3)_2{\cdot}6H_2O$ and 0.5 M citric acid were dissolved in ethanol (25 mL) and deionised water (25 mL). The mixture was stirred at 90 °C in a 500 mL round bottom flask placed in a silicon oil bath. The salt mixture was stirred vigorously and evaporation resulted in the formation of a transparent sol. This was dried at 60 °C for 12 h and calcined at 400 °C for 5 h. The catalyst synthesised was denoted as SG-$La_2O_2CO_3$.

3.3. Catalyst Characterisation

Scanning electron microscopy (SEM) (JEOL JSM-6010LA; JEOL, Tokyo, Japan) was employed to study the morphology of the catalyst. The total surface area of catalysts was evaluated using Brunauer Emmett Teller (BET) measurements (Micromeritics 3-Flex; Micromeritics, Lincoln UK): 0.5 g catalyst was loaded into the sample tube and degassed 250 °C for 3 h prior to analysis using Vac Prep 061 (Micromeritics, Norcross, GA, USA). Surface functionalities have been analysed using a Fourier transform infrared spectrometer (FTIR) (Shimadzu IRAffinity-IS; Shimadzu, Kyoto, Japan) measuring over the range 400 to 4000 cm^{-1}. The oxide phase was characterised via X-ray diffraction (D2 Phaser Bruker Ltd.; Coventry, UK) employing CuKα1 radiation (λ = 1.5406 Å). A graphite monochromator was maintained at a tube voltage and current of 30 kV and 10 mA respectively. QuantaChrome ChemBet Pulsar/TPR (Boynton Beach, FL, USA) equipped with a thermal conductivity

detector was employed to perform TPD-CO_2 analysis. 0.1 g of catalyst was placed in a U shaped quartz reactor. The catalyst was then pre-treated using He at 300 °C for 1 h and before being cooled to 30 °C. The sample was then treated with flowing pure CO_2 for 1 h before purging with He to remove physisorbed CO_2. The temperature was increased from 30 to 900 °C with a heating ramp of 10 °C min^{-1}.

3.4. Catalytic Testing

The direct carboxylation of glycerol with CO_2 was carried out in a 45 mL stainless steel autoclave (Parr Instruments, Model 4714; Parr Instruments, Moline, IL, USA). 22.5 mmol of glycerol, 45 mmol dehydrating agent and 6 wt.% catalyst to glycerol ratio were loaded into the reactor and stirred using a magnetic stirrer. The reactor was purged and cycled with 20 bar CO_2. Then, 34 bar CO_2 was introduced to the reactor at room temperature. The reaction temperature was set at 160 °C and the reaction was carried out for 18 h.

3.5. Liquid-Phase Products Analysis

ATR-FTIR analysis was conducted employing a Shimadzu IRAfinity-1S (Kyoto, Japan). The spectra were collected from 400 to 4000 cm^{-1} with a resolution of 4 cm^{-1}. The liquid-phase resulting from reaction was placed directly onto the ATR plate. Gas chromatography-mass spectrometry (Shimadzu GCMSQP2012SE; Shimadzu, Kyoto, Japan) equipped with a 30 m HP-Innowax capillary column was also employed to analyse the composition of the liquid products. Ethanol was used as the solvent. Stock solutions of glycerol, glycerol carbonate, mono-, di- and triacetin were prepared for calibration in order to allow for quantitative analysis. Glycerol conversion and the selectivity to glycerol carbonate and by-products including mono-, di- and triacetin were calculated as follows:

$$\%\ conversion = 100 \times \left(\frac{moles\ of\ glycerol\ consumed}{moles\ of\ glycerol\ introduced} \right) \quad (1)$$

$$\%\ selectivity = 100 \times \left(\frac{moles\ of\ products\ formed}{moles\ of\ glycerol\ consumed} \right) \quad (2)$$

4. Conclusions

In this work, the catalytic upgrading of glycerol in the presence of lanthanum-based catalysts and dehydrating agents has been investigated. In general, acidic dehydrating agents promote acetin formation, whereas basic dehydrating agents promote glycerol carbonate formation. Acetins can however also be formed in the presence of basic species through secondary reactions. Notably, conducting the reaction in the presence of adiponitrile results in a 5-fold increase in glycerol carbonate yield when compared to acetonitrile, which is currently the most commonly applied dehydrating agent. This effect is in part ascribed to the dicyanated structure of adiponitrile. However, other factors such as limiting alternative reaction pathways leading to the production of undesired by-products and mass transfer effects through changes in CO_2 solubility also play key roles. It is therefore anticipated that the application of adiponitrile in the presence of optimized catalysts would lead to improvements in this field. The use of a lanthanum-based catalyst in this work allows for correlation to be drawn with previous studies. In addition, the influence of catalyst preparation method has been investigated. Catalyst synthesis has a profound effect on the crystalline phase formed and therefore on catalyst performance. Together, these novel insights provide a clear route for the optimisation of glycerol carboxylation reactions to produce value-added products.

Supplementary Materials: The following are available online at https://www.mdpi.com/2073-4344/11/1/138/s1, Figure S1: Particle size distributions for (a) CP-$La_2O_2CO_3$ and (b) HT-$La_2O_2CO_3$ determined from analysis of multiple SEM micrographs, Table S1: Mass spectrometry fragmentation pattern of unidentified product (chromatogram retention time = 35.5 min) identified from the carboxylation of glycerol in the presence of benzonitrile as a dehydrating agent, Table S2: Influence of

the dehydrating agents on by-product formation, Table S3: Influence of catalyst synthesis method on by-product formation.

Author Contributions: All authors contributed equally to this work. All authors have read and agreed to the published version of the manuscript.

Funding: The authors acknowledge support via EPSRC grant EP/R026815/1 and via EP/K001329/1.

Institutional Review Board Statement: Not applicable.

Informed Consent Statement: Not applicable.

Data Availability Statement: The data presented in this study are openly available in the White Rose repository, identification number uk.bl.ethos.736566: http://etheses.whiterose.ac.uk/19350/.

Acknowledgments: The University of Manchester is thanked for TPD analysis.

Conflicts of Interest: The authors declare no conflict of interest. The funders had no role in the design of the study; in the collection, analyses, or interpretation of data; in the writing of the manuscript, or in the decision to publish the results.

References

1. Razali, N.A.; Conte, M.; McGregor, J.M. The role of impurities in the La_2O_3 catalysed carboxylation of crude glycerol. *Catal. Lett.* **2019**, *149*, 1403–1414. [CrossRef]
2. Ciriminna, R.; Della Pina, C.; Rossi, M.; Pagliaro, M. Understanding the glycerol market. *Eur. J. Lipid Sci. Technol.* **2014**, *116*, 1432–1439. [CrossRef]
3. Sonnati, M.O.; Amigoni, S.; De Givenchy, E.P.T.; Darmanin, T.; Choulet, O.; Guittard, F. Glycerol carbonate as a versatile building block for tomorrow: Synthesis, reactivity, properties and applications. *Green Chem.* **2013**, *15*, 283–306. [CrossRef]
4. Konwar, L.J.; Mäki-Arvela, P.; Begum, P.; Kumar, N.; Thakur, A.J.; Mikkola, J.-P.; Deka, R.C.; Deka, D. Shape selectivity and acidity effects in glycerol acetylation with acetic anhydride: Selective synthesis of triacetin over Y-zeolite and sulfonated mesoporous carbons. *J. Catal.* **2015**, *329*, 237–247. [CrossRef]
5. Sandesh, S.; Manjunathan, P.; Halgeri, A.B.; Shanbhag, G.V. Glycerol acetins: Fuel additive synthesis by acetylation and esterification of glycerol using cesium phosphotungstate catalyst. *RSC Adv.* **2015**, *5*, 104354–104362. [CrossRef]
6. Kong, P.S.; Aroua, M.K.; Daud, W.M.A.W.; Lee, H.V.; Cognet, P.; Pérès, Y. Catalytic role of solid acid catalysts in glycerol acetylation for the production of bio-additives: A review. *RSC Adv.* **2016**, *6*, 68885–68905. [CrossRef]
7. Shapira, J.; Mandel, A.D.; Quattrone, P.D.; Bell, N.L. Current research on regenerative systems. *Life Sci. Space Res.* **1969**, *7*, 123–129.
8. Alper, E.; Orhan, O.Y. CO_2 utilization: Developments in conversion processes. *Petroleum* **2017**, *3*, 109–126. [CrossRef]
9. Narkhede, N.; Patel, A. Facile synthesis of glycerol carbonate via glycerolysis of urea catalysed by silicotungstates impregnated into MCM-41. *RSC Adv.* **2015**, *5*, 52801–52808. [CrossRef]
10. DiBenedetto, A.; Angelini, A.; Aresta, M.; Ethiraj, J.; Fragale, C.; Nocito, F. Converting wastes into added value products: From glycerol to glycerol carbonate, glycidol and epichlorohydrin using environmentally friendly synthetic routes. *Tetrahedron* **2011**, *67*, 1308–1313. [CrossRef]
11. Indran, V.P.; Zuhaimi, N.A.S.; Deraman, M.A.; Maniam, G.P.; Yusoff, M.M.; Hin, T.-Y.Y.; Rahim, M.H.A. An accelerated route of glycerol carbonate formation from glycerol using waste boiler ash as catalyst. *RSC Adv.* **2014**, *4*, 25257–25267. [CrossRef]
12. Hammond, C.; Lopez-Sanchez, A.J.; Ab Rahim, M.H.; Dimitratos, N.; Jenkins, L.R.; Carley, F.A.; He, Q.; Kiely, J.C.; Knight, W.D.; Hutchings, G.J. Synthesis of glycerol carbonate from glycerol and urea with gold-based catalysts. *Dalt. Trans.* **2011**, *40*, 3927–3937. [CrossRef] [PubMed]
13. Climent, M.J.; Corma, A.; De Frutos, P.; Iborra, S.; Noy, M.; Velty, A.; Concepción, P. Chemicals from biomass: Synthesis of glycerol carbonate by transesterification and carbonylation with urea with hydrotalcite catalysts. The role of acid–base pairs. *J. Catal.* **2010**, *269*, 140–149. [CrossRef]
14. Algoufi, Y.; Akpan, U.; Kabir, G.; Asif, M.; Hameed, B. Upgrading of glycerol from biodiesel synthesis with dimethyl carbonate on reusable Sr–Al mixed oxide catalysts. *Energy Convers. Manag.* **2017**, *138*, 183–189. [CrossRef]
15. Simanjuntak, F.S.H.; Widyaya, V.T.; Kim, C.S.; Ahn, B.S.; Mishra, V.; Lee, H. Synthesis of glycerol carbonate from glycerol and dimethyl carbonate using magnesium–lanthanum mixed oxide catalyst. *Chem. Eng. Sci.* **2013**, *94*, 265–270. [CrossRef]
16. Rahim, M.H.A.; He, Q.; Lopez-Sanchez, J.A.; Hammond, C.; Dimitratos, N.; Sankar, M.; Carley, A.F.; Kiely, C.J.; Knight, D.W.; Hutchings, G.J. Gold, palladium and gold–palladium supported nanoparticles for the synthesis of glycerol carbonate from glycerol and urea. *Catal. Sci. Technol.* **2012**, *2*, 1914–1924. [CrossRef]
17. Su, X.; Lin, W.; Cheng, H.; Zhang, C.; Wang, Y.; Yu, X.; Wu, Z.; Zhao, F. Metal-free catalytic conversion of CO_2 and glycerol to glycerol carbonate. *Green Chem.* **2017**, *19*, 1775–1781. [CrossRef]
18. Collett, C.; Mašek, O.; Razali, N.; McGregor, J.M. Influence of Biochar Composition and Source Material on Catalytic Performance: The Carboxylation of Glycerol with CO_2 as a Case Study. *Catalysts* **2020**, *10*, 1067. [CrossRef]

19. CO_2 Now the Most Current CO_2 Data on Earth. Available online: http://co2now.org/Current-CO2/CO2-Now/global-co2-board.html (accessed on 1 July 2020).
20. Li, J.; Wang, T. Coupling reaction and azeotropic distillation for the synthesis of glycerol carbonate from glycerol and dimethyl carbonate. *Chem. Eng. Process. Process Intensif.* **2010**, *49*, 530–535. [CrossRef]
21. Li, J.; Wang, T. Chemical equilibrium of glycerol carbonate synthesis from glycerol. *J. Chem. Thermodyn.* **2011**, *43*, 731–736. [CrossRef]
22. Ozorio, L.P.; Pianzolli, R.; Machado, L.D.C.; De Miranda, J.L.; Turci, C.C.; Guerra, A.; Souza-Aguiar, E.F.; Mota, C.J.A. Metal-impregnated zeolite Y as efficient catalyst for the direct carbonation of glycerol with CO_2. *Appl. Catal. A Gen.* **2015**, *504*, 187–191. [CrossRef]
23. Ozorio, L.P.; Mota, C.J.A. Direct Carbonation of Glycerol with CO_2 Catalyzed by Metal Oxides. *ChemPhysChem* **2017**, *18*, 3260–3265. [CrossRef] [PubMed]
24. George, J.; Patel, Y.; Pillai, S.M.; Munshi, P. Methanol assisted selective formation of 1,2-glycerol carbonate from glycerol and carbon dioxide using nBu_2SnO as a catalyst. *J. Mol. Catal. A Chem.* **2009**, *304*, 1–7. [CrossRef]
25. Li, H.; Xin, C.; Jiao, X.; Zhao, N.; Xiao, F.; Li, L.; Wei, W.; Sun, Y. Direct carbonylation of glycerol with CO_2 to glycerol carbonate over Zn/Al/La/X (X=F, Cl, Br) catalysts: The influence of the interlayer anion. *J. Mol. Catal. A Chem.* **2015**, *402*, 71–78. [CrossRef]
26. Li, H.; Gao, D.; Gao, P.; Wang, F.; Zhao, N.; Xiao, F.; Wei, W.; Sun, Y. The synthesis of glycerol carbonate from glycerol and CO_2 over $La_2O_2CO_3$–ZnO catalysts. *Catal. Sci. Technol.* **2013**, *3*, 2801–2809. [CrossRef]
27. Li, H.; Jiao, X.; Li, L.; Zhao, N.; Xiao, F.; Wei, W.; Sun, Y.; Zhang, B. Synthesis of glycerol carbonate by direct carbonylation of glycerol with CO_2 over solid catalysts derived from Zn/Al/La and Zn/Al/La/M (M = Li, Mg and Zr) hydrotalcites. *Catal. Sci. Technol.* **2014**, *5*, 989–1005. [CrossRef]
28. Zhang, J.; He, D. Synthesis of glycerol carbonate and monoacetin from glycerol and carbon dioxide over Cu catalysts: The role of supports. *J. Chem. Technol. Biotechnol.* **2014**, *90*, 1077–1085. [CrossRef]
29. Zhang, J.; He, D. Surface properties of Cu/La2O3 and its catalytic performance in the synthesis of glycerol carbonate and monoacetin from glycerol and carbon dioxide. *J. Colloid Interface Sci.* **2014**, *419*, 31–38. [CrossRef]
30. Liu, J.; Li, Y.; Zhang, J.; He, D. Glycerol carbonylation with CO_2 to glycerol carbonate over CeO_2 catalyst and the influence of CeO2 preparation methods and reaction parameters. *Appl. Catal. A Gen.* **2016**, *513*, 9–18. [CrossRef]
31. Park, C.-Y.; Nguyen-Phu, H.; Shin, E.W. Glycerol carbonation with CO_2 and La_2O_2 CO_3/ZnO catalysts prepared by two different methods: Preferred reaction route depending on crystalline structure. *Mol. Catal.* **2017**, *435*, 99–109. [CrossRef]
32. Zhou, Q.; Zhang, H.; Chang, F.; Li, H.; Pan, H.; Xue, W.; Hu, D.-Y.; Yang, S. Nano La_2O_3 as a heterogeneous catalyst for biodiesel synthesis by transesterificatiob of Jatropha curcas L. oil. *J. Ind. Eng. Chem.* **2015**, *31*, 385–392. [CrossRef]
33. Abboudi, M.; Messali, M.; Kadiri, N.; Ben Ali, A.; Moran, E. Synthesis of CuO, La_2O_3, and La_2CuO_4 by the Thermal-Decomposition of Oxalates Precursors Using a New Method. *Synth. React. Inorg. Met. Chem.* **2011**, *41*, 683–688. [CrossRef]
34. Wang, X.; Wang, M.; Song, H.; Ding, B. A simple sol–gel technique for preparing lanthanum oxide nanopowders. *Mater. Lett.* **2006**, *60*, 2261–2265. [CrossRef]
35. Pons, A.; Jouin, J.; Bechade, E.; Julien, I.; Masson, O.; Geffroy, P.M.; Mayet, R.; Thomas, P.; Fukuda, K.; Kagomiya, I. Study of the formation of the apatite-type phases $La9.33+x(SiO_4)_6O_2+3x/2$ synthesized from a lanthanum oxycarbonate $La_2O_2CO_3$. *Solid State Sci.* **2014**, *38*, 150–155. [CrossRef]
36. Valange, S.; Beauchaud, A.; Barrault, J.; Gabelica, Z.; Daturi, M.; Can, F. Lanthanum oxides for the selective synthesis of phytosterol esters: Correlation between catalytic and acid–base properties. *J. Catal.* **2007**, *251*, 113–122. [CrossRef]
37. Mu, Q.; Wang, Y. Synthesis, characterization, shape-preserved transformation, and optical properties of $La(OH)_3$, $La_2O_2CO_3$, and La_2O_3 nanorods. *J. Alloy Compd.* **2011**, *509*, 396–401. [CrossRef]
38. Gangwar, B.P.; Palakollu, V.; Singh, A.; Kanvah, S.; Sharma, S. Combustion synthesized $La_2O_3$and $La(OH)_3$: Recyclable catalytic activity towards Knoevenagel and Hantzsch reactions. *RSC Adv.* **2014**, *4*, 55407–55416. [CrossRef]
39. Da Silva, E.; Dayoub, W.; Mignani, G.; Raoul, Y.; Lemaire, M. Propylene carbonate synthesis from propylene glycol, carbon dioxide and benzonitrile by alkali carbonate catalysts. *Catal. Commun.* **2012**, *29*, 58–62. [CrossRef]
40. Saiyong, P.; Liping, Z.; Renfeng, N.; Shuixin, X.; Ping, C.; Zhaoyin, H. Transesterification of Glycerol with Dimethyl Carbonate to Glycerol Carbonate over Na–based Zeolites. *Chin. J. Catal.* **2012**, *33*, 1772–1777.
41. Yang, J.; Zhao, Q.; Xu, H.; Li, L.; Dong, J.; Li, J. Adsorption of CO_2, CH_4, and N_2 on Gas Diameter Grade Ion-Exchange Small Pore Zeolites. *J. Chem. Eng. Data* **2012**, *57*, 3701–3709. [CrossRef]
42. Silva, L.N.; Gonçalves, V.L.; Mota, C.J.A. Catalytic acetylation of glycerol with acetic anhydride. *Catal. Commun.* **2010**, *11*, 1036–1039. [CrossRef]
43. Liao, X.; Zhu, Y.; Wang, S.-G.; Chen, H.; Li, Y. Theoretical elucidation of acetylating glycerol with acetic acid and acetic anhydride. *Appl. Catal. B Environ.* **2010**, *94*, 64–70. [CrossRef]
44. Shimizu, K.-I.; Kon, K.; Onodera, W.; Yamazaki, H.; Kondo, J.N. Heterogeneous Ni Catalyst for Direct Synthesis of Primary Amines from Alcohols and Ammonia. *ACS Catal.* **2012**, *3*, 112–117. [CrossRef]